The complexity of water freezing under reduced atmospheric pressure

Petr Brož[1*], Vojtěch Patočka[2], Frances Butcher[3], Matthew Sylvest[4], and Manish Patel[4,5]

[1] Institute of Geophysics of the Czech Academy of Sciences, Prague, Czech Republic, petr.broz@ig.cas.cz

[2]Charles University, Faculty of Mathematics and Physics, Department of Geophysics, Prague, Czech Republic

[3]School of Geography and Planning, University of Sheffield, Sheffield, UK

[4] School of Physical Science, STEM, The Open University, Milton Keynes, UK

[5] Space Science and Technology Department, STFC Rutherford Appleton Laboratory, Oxford, UK

* Corresponding author

Citation: Brož, P., Patočka, V., Butcher, F., Sylvest, M., & Patel, M. (2025). The complexity of water freezing under reduced atmospheric pressure. *Earth and Planetary Science Letters, 668*, 119531.

https://doi.org/10.1016/j.epsl.2025.119531

Highlights

- Subsurface boiling affects the rate and manner of ice freezing under low pressure
- Ice deformation and cracking result from ascending vapour beneath the ice layer
- Pressure release triggers repeated cycles of boiling, bubble formation, and cracking
- Fracturing and vapour build-up create uneven surfaces with centimetre-scale features
- Cryolava ponds and flows may preserve complex signatures of solidification dynamics

Abstract

The surfaces of many icy bodies in the Solar System have been resurfaced by cryovolcanism, during which liquid and vapour are released from the subsurface into cold, near-vacuum conditions. Water is one of the most commonly released liquids, but it is not stable at low pressure – boiling near the water surface causes rapid cooling and induces surface freezing. Despite previous theoretical works and laboratory experiments it remains unclear how the three coexisting phases interact. Here we expose large volumes of liquid water (17 and 5 litres) to low pressure to study how the phase transitions interact in the near-surface layer, and what controls the dynamics of the system. We observe that subsurface boiling and associated bubble formation significantly affects the rate and manner of freezing. Ascending vapour deforms the ice and causes it to crack, which releases subsurface pressure. Once the pressure is released, the underlying liquid water is again exposed to the reduced atmospheric pressure, triggering a new cycle of vigorous boiling, bubble formation, ice deformation, and subsequent cracking. Thereby, the period of boiling and freeze-over is prolonged. Additionally, we observe that fracturing and vapour accumulation beneath the ice layer create an uneven surface, characterized by bumps and depressions a few centimetres in height. This shows that ice solidification during effusive cryovolcanic eruptions is likely to be a highly complex process and could leave distinct, observable signatures on and within cryolava ponds and flows.

1. Introduction

Signs of past or active cryovolcanism have been observed on Europa, Titan, Enceladus, Triton, Pluto and Ceres (e.g., Kirk et al., 1995; Porco et al., 2006; Roth et al., 2014; Küppers et al., 2014; Ruesch et al., 2019). Cryovolcanic worlds have been identified as high-priority targets (Hendrix et al., 2019) from which to learn about subsurface chemistry and possible habitability. While signs of explosive cryovolcanism, including active plumes, have been observed on Enceladus, Triton, and likely also on Europa (e.g., Sparks et al., 2017), evidence for effusive cryovolcanism is rarer and harder to detect (e.g., Fagents, 2003; Lopes et al., 2007; Lesage et al, 2021). The best examples are from Europa, where domes and smooth, ice-rich, low-albedo surfaces infill low-lying areas (e.g., Fagents, 2003). However, since these features formed millions to billions years ago (e.g., Strom, 1986; Kargel, 1994; McGovern et al., 2021) and no active cryolava flows have been observed, it remains unclear how effusive cryovolcanism actually operates, limiting our ability to identify its imprints and products on icy moons.

Previously, it was proposed that effusive cryovolcanic features might share morphological similarities to terrestrial volcanic features (e.g., Fagents, 2003). However, theory and experiments show liquid water experiences double instability in vacuum-like environments (e.g., Bargery et al., 2010; Quick et al., 2017; Brož et al., 2020a; 2023; Poston et al., 2024). Significant differences are thus expected between terrestrial and cryovolcanic lavas, as well as mud flows and ponded water bodies in low pressure environments (e.g., Allison and Clifford, 1987; Brož et al., 2020a,b; 2023; Ahrens, 2020; Morrison et al., 2022; Poston et al., 2024; Krýza et al., 2025).

Previous laboratory experiments have worked with small liquid water volumes water (<500 ml) in small tubes (<2 cm radius) and thus were severely limited by the imposed boundary conditions (Bargery et al., 2010), or unable to show the processes taking place in a deeper water column (Brož et al., 2020a,b; 2023; Poston et al., 2024). Moreover, these experiments were conducted at temperatures significantly higher than those expected on icy moons or Mars, limiting their applicability to real planetary environments. This leaves many uncertainties about the behaviour of liquid water as it both freezes and boils at low pressure, in particular, how stable the ice crust is with respect to the forces that act to disrupt it. These include the buoyancy of coalescing bubbles in the early stage of freezing, the disruptive flow of the eruptive cryofluid, and pressurization due to the ice/water density contrast in the later stages when the underlying liquid water is effectively sealed. The possible end-member scenarios are vastly different: either the crust is unstable, being repeatedly fractured and allowing the release of large volumes of vapour to space, or the crust quickly gains sufficient strength to seal the liquid (e.g., Umurhan et al., 2021) and impede its further propagation or loss. As direct observational insights from nature are missing, we performed two analogue experiments to study the critical moment when liquid water is subjected to low atmospheric pressure and begins to freeze.

2. Experimental setup

We conducted experiments using the Mars Simulation Chamber at The Open University (UK). A 60 × 40 cm plastic tank was filled with 17 and 5 litres of liquid water ('Exp1' and 'Exp2'; water depths ~7 and 2 cm respectively). The effusion of pure water from planetary subsurfaces is unlikely, so NaCl was mixed with deionized water to achieve a salinity of 0.5%. The water was precooled to ~3.8°C (in Exp1) and 6.4°C (in Exp2) respectively to simulate low temperatures of effusive cryoeruptions. The experiment was documented using a camera above the tank and another providing an angled side view, and three thermocouples to monitor the water and air temperatures inside the chamber (Fig. 1). The atmospheric pressure was gradually reduced from 1 bar to ~4.5 mbar, where it oscillated between 4.5 and 4.7 mbar due to the opposing effects of vacuum pump performance and vapour production. After each experiment was completed and the chamber was re-pressurized to ambient conditions, we weighed the remaining liquid water to reveal its loss due to evaporation and sublimation.

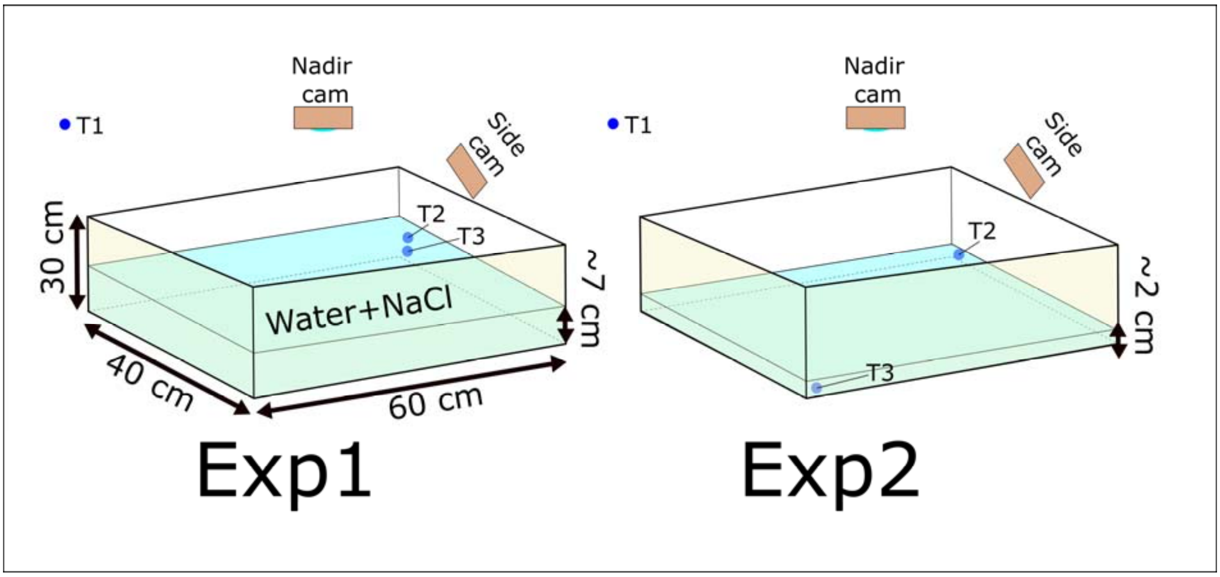

Figure 1: Illustration of the experimental setup inside the Mars Simulation Chamber. Note the positions of thermocouples used to monitor temperature inside the chamber (T1) and water tank (T2 and T3, placed at the depths of 1.5 and 5 cm in Exp1).

3. Observations

The gradual pressure reduction at the beginning of both experiments caused water degassing (for details see movies in Supplementary material [low-res version] on Zenodo [high-res version], Brož et al., 2025). Escape of sub-mm-sized bubbles caused small visible disturbances on the water surface (Fig. 2a,j). When the chamber pressure reached the saturated vapour pressure, the water began to boil. Initially, bubbles were mm-sized (Fig. 2b), but quickly reached cm-size (Fig. 2d) as the depth of boiling increased to a few cm over ~50 s (Fig. 3a,c), producing a large amount of water vapour. In both experiments, rapid bubble formation repeatedly disturbed the water surface, ejecting droplets. While the setup did not permit direct quantification of material loss, post-experiment weighing revealed ~1173 g and ~150 g escaped during Exp1 and Exp2, respectively. During Exp1, ~7% of the 17 litres of water was lost, compared to 3% of 5 litres in Exp2, indicating that the water layer in Exp2 was too shallow to accurately capture all of the studied processes.

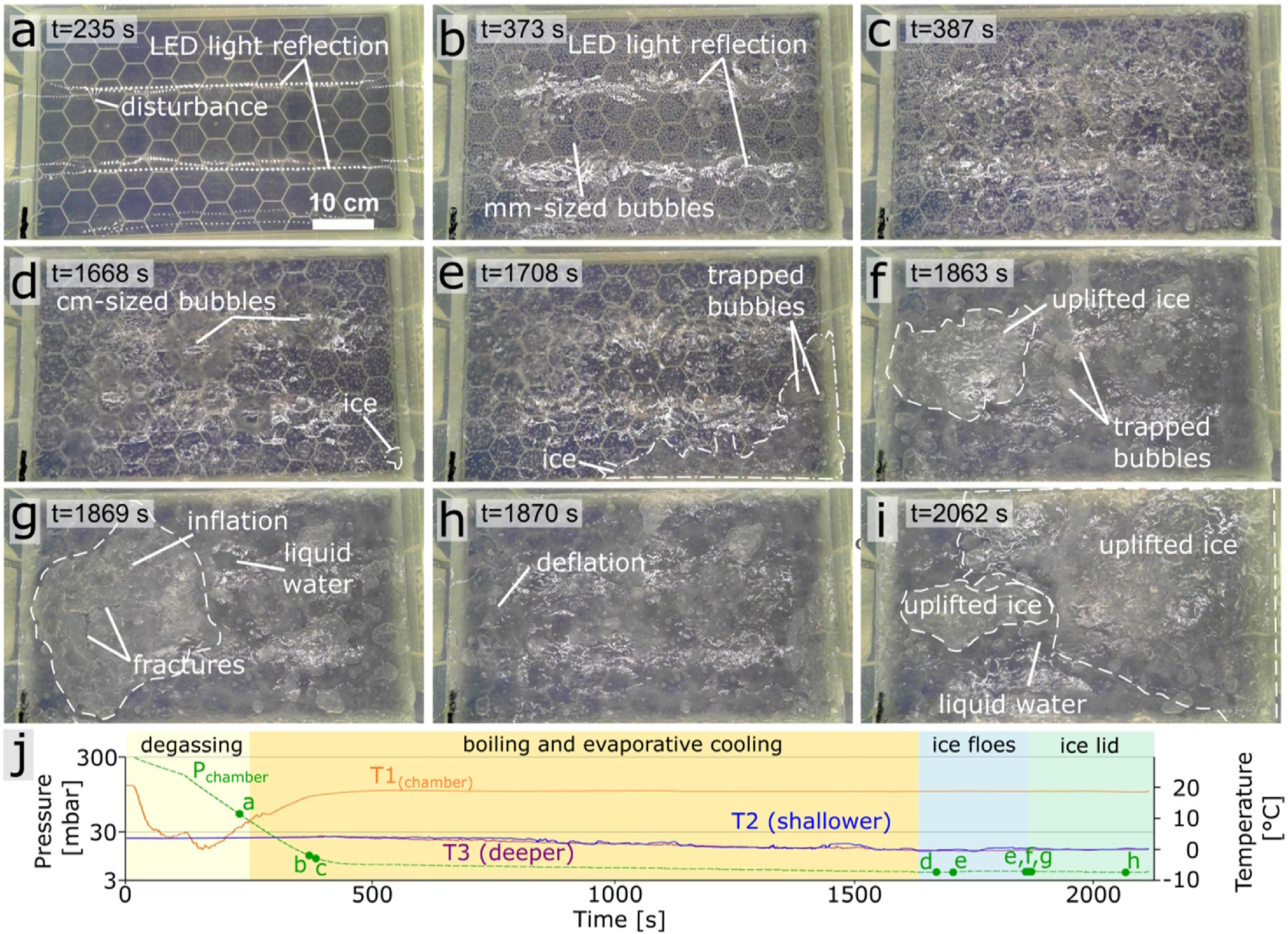

a t=235 s
LED light reflection
disturbance
10 cm
b t=373 s
LED light reflection
mm-sized bubbles
c t=387 s
d t=1668 s
cm-sized bubbles
ice
e t=1708 s
trapped bubbles
ice
f t=1863 s
uplifted ice
trapped bubbles
g t=1869 s
inflation
liquid water
fractures
h t=1870 s
deflation
i t=2062 s
uplifted ice
uplifted ice
liquid water
j
degassing
boiling and evaporative cooling
ice floes
ice lid
P chamber
T1 (chamber)
T2 (shallower)
T3 (deeper)
a
b
c
d
e
e,f,g
h
Pressure [mbar]
300
30
3
Temperature [°C]
20
10
0
-10
0
500
1000
1500
2000
Time [s]

*Figure 2: (a-i) Snapshots from various time points of movie capturing Exp1 (a-i) illustrating the behaviour of liquid water under low atmospheric pressure. Note the deflation of the uplifted area, which occurs When pressure dropped below the saturated vapour pressure (j), vigorous boiling began, reducing the temperature to the freezing point. Floating ice formed and gradually covered the tank, but continued boiling fractured and lifted the ice crust, delaying full surface freezing. See accompanying movie in the external repository for details. The green dots with letters at panel (j) correspond with subpanels (a-i). The above referred movie can be seen in low-resolution format in Supplementary material or downloaded in full-resolution from Zenodo (*https://zenodo.org/records/14639337).

Removal of the latent heat of vaporization cooled the water column in both experiments; in each case, its temperature followed the phase change boundary, maintaining equilibrium as the chamber pressure reduced (Fig. 3a). In an Earth-like environment, near solidus (<4° C), liquid water bodies cooled from above develop a stable thermal boundary layer because the density decreases towards the cold surface. In our low-pressure experiments, ascending bubbles disrupted this layer, promoting mixing to greater depths. As a result, the temperature decreased nearly uniformly in the bulk of the liquid water (Fig. 3b), despite vaporization being the strongest near the surface.

In the following two paragraphs, we describe the temporal evolution observed in Exp1; however, the same behaviour — with different timing — was also observed in Exp2 (see Tab. 1 for details). After ~1320 s of boiling (Fig. 2j), the liquid water temperature reached the freezing point and floating ice pieces formed (Fig. 2d). Thereafter, the ice-covered area gradually increased as new ice pieces formed and the existing ones grew at the edges (Fig. 2e). Within a few minutes, most of the liquid water surface was ice-covered (Fig. 2f, j). However, the layer was not intact, but was instead cracked with some patches of liquid water on the ice surface. (Fig. 2g). This occurred because boiling continued beneath the freezing layer, generating vapour pockets that broke or lifted sections of the ice, and allowed liquid to effuse onto the ice surface. Such a behaviour is different from the Bargery et al. (2010) small-tube experiments, in which rapid formation of a mechanically strong layer led to a sudden cessation of boiling events.

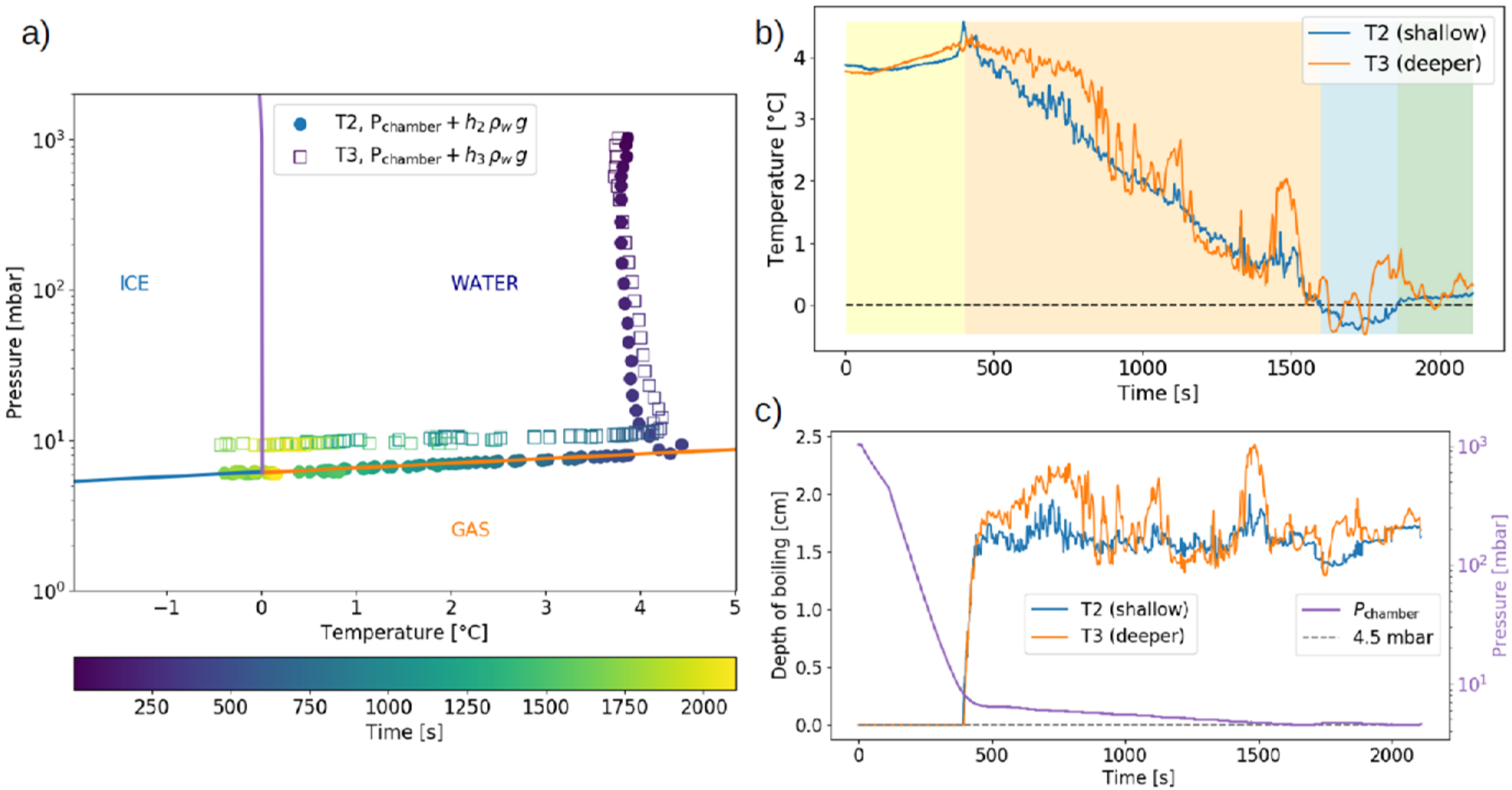
a)
T2, $P_{chamber} + h_2 \rho_w g$
T3, $P_{chamber} + h_3 \rho_w g$
ICE
WATER
GAS
Pressure [mbar]
Temperature [°C]
Time [s]
b)
T2 (shallow)
T3 (deeper)
Temperature [°C]
Time [s]
c)
T2 (shallow)
T3 (deeper)
$P_{chamber}$
4.5 mbar
Depth of boiling [cm]
Pressure [mbar]
Time [s]

Figure 3: (a) Path of Exp1 in the P,T phase diagram. Circles and squares show the temperature at T2 and T3 combined with the idealized assumption of hydrostatic pressure, $P_{chamber} + h\ \rho_{purewater}\ g$, where h=1.5 and 5.0 cm are the thermocouple depths; colour shows time. (b) Temperatures at T2 and T3 through Exp1 (yellow marks the degassing phase, orange the boiling and evaporative cooling phase, blue the ice floes phase, and green the ice lid phase respectively). (c) Estimated minimum depth of boiling for the two temperature evolutions: $(P_{SV} - P_{chamber}) / (\rho_{purewater}\ g)$, where P_{SV} is the saturated vapour pressure computed as a function of temperature.

#	Volume of water [l]	Water temperature [°C]	Water surface height [cm]	Duration of experiment [min:sec]	Occurrence of the first ice [sec]	End of ice lid formation phase [sec]	Post experiment mass loss [g]
Exp1	12	3.8	7	35:13	27:30	31:20	1173
Exp2	5	6.4	2	30:51	20:40	25:40	150

Table 1: Summary of key data describing the sequence and conditions of the two experimental runs.

Boiling was more vigorous in Exp1 than in Exp2, indicating that the boiling depth in Fig. 3c is only the lower estimate, because $\rho = \rho_{purewater}$ was used to compute hydrostatic pressure while the boiling layer has a lower density. Once fractures appeared, trapped vapour was released, causing deflation and liquid effusion over the ice crust (Fig. 2h). The amount of vapour trapped beneath the ice varied, leading to different degrees of uplift (Fig. 2i). Lifting and cracking of the ice layer, accompanied by boiling, continued for ten minutes (Fig. 2j) before the experiment was terminated due to large amounts of water vapour escaping into the oil pumps. Inspection of the ice crust after the chamber was pressurized revealed that in the case of both experiments, the ice crust was not smooth, as would be typical under ambient pressure, but instead was uneven, with ~cm high undulations. Throughout the experiments, the ice remained transparent and did not turn `snow-like' nor form frazil ice (the type of ice characterized by small, loose, needle-like ice crystals suspended in water) as observed in the Bargery et al. (2010) experiments.

4. Discussion and conclusions

With reference to potential effusive cryolava on Jupiter's moon Ganymede, Allison and Clifford (1987) proposed that exposure of liquid water to the cold, vacuum-like environment would lead to intense boiling in the bulk of the fluid as the saturated vapour pressure would exceed the ambient pressure. This was confirmed experimentally, when ~90 ml of liquid water was exposed to martian pressure (Bargery et al., 2010). Allison and Clifford (1987) also proposed that an icy crust would develop due to freezing at the surface and base of a cryovolcanic flow, but that continuous vapour formation during freezing would repetitively disrupt this icy crust. Our experiments show this process in action, and illustrate the contributing factors (Fig. 4).

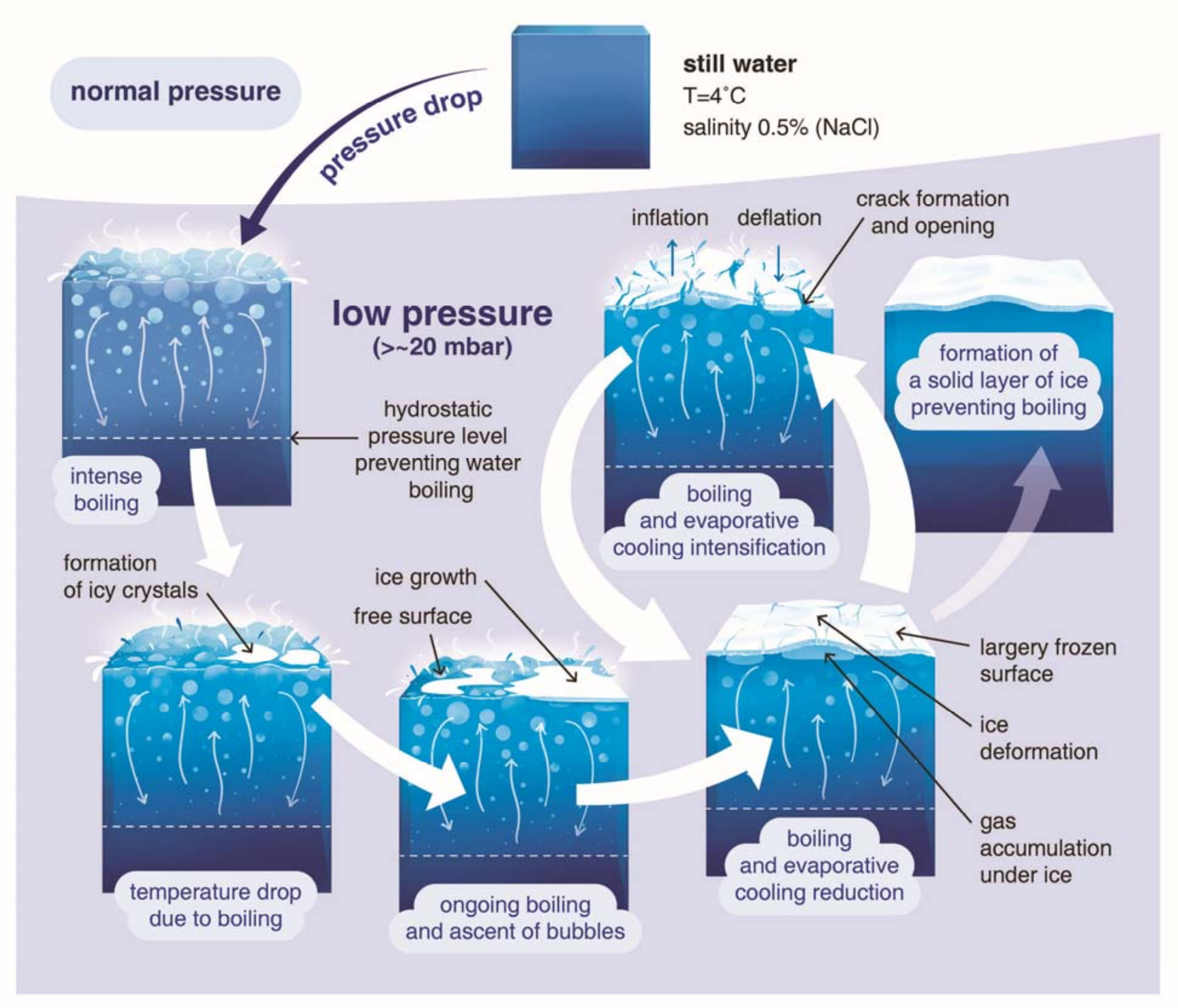

Figure 4: Schematic model showing the main phases associated with the phase transition of water under reduced atmospheric pressure.

An important role is played by rising bubbles which mix the liquid water and disrupt the shallow thermal boundary layer. Mixing delays the onset of surface freezing (Morrison et al., 2022). The boiling also affects how the water surface freezes. Under terrestrial pressure, ice crystals would gradually grow and coalesce until they cover the entire surface of the water (e.g., Ashton, 1986), whereas our experiments showed different dynamics. Bubbles transported ice crystals to various sites, where they merged into small ice pieces. These pieces were moved from side to side by bubbles, which also broke off ice fragments and pushed the broken edges around (See Movies in Supplementary materials or on Zenodo for details). Ice fragments and crystals act as nucleation sites; they grow and merge until a continuous ice cover forms (ice lid stage, Fig. 2j).

Since both vapour and ice are less dense than liquid water, the phase changes in a sealed liquid water body should lead to pressurisation that eventually halts boiling. The experiment's duration was insufficient to determine when the ice layer would eventually stabilize and prevent further loss of material. Allison and Clifford (1987) theorized that in the case of Ganymede boiling stops when ice thickness exceeds ~0.5 meters, insulating the liquid from the vacuum. Quick et al. (2017) calculated that Europa's cryolavas could form such ice crusts within 7.5 days. Hydrostatic pressure rises faster with depth under higher gravity on Earth, limiting the boiling depth in our experiments compared to low-gravity environments in the Solar System, where the depth of the boiling column could be several metres (1.5 cm in Fig. 3c implies ca. 1.3 m on Enceladus, cf. also Fig. 10 in Brož et al., 2023). Deeper boiling during real cryovolcanic eruptions would imply a higher vapour production rate, resulting in more and larger bubbles, which is the key disruptive force that determines how quickly the surface gets sealed.

As sublimation is much less effective at extracting heat than boiling (by ~5 times, Bargery et al., 2010), the ice growth is slow once boiling ceases. Formation of a continuous ice cover is thus a critical moment in the evolution of the system, and here we illustrate for the first time how the lid may behave on a large scale (Figs. 2 and 4). On one hand, the heat of sublimation is ca. 8.5 times greater than the heat of fusion, which means that ice should grow into the liquid water faster than the upper surface can sublime, building a stable solid layer (Bargery et al., 2010). On the other hand, once bubbles cannot escape freely, they accumulate below the lid (Raposa et al., 2024). Large bubbles locally elevate the ice, attracting trapped bubbles from a broader area, merging into a pocket of vapour below thin, flexed ice. These pockets were able to repetitively crack the ice and escape, levelling the topography and spilling liquid water onto the ice surface (Fig. 2). When near the edge of the tank, the pockets would escape by lifting the ice at the wall of the container. In other words, thermal pathways through the ice are more numerous than previously thought.

4.1. Experimental limitations

Our experiments have several important deviations from actual cryovolcanic conditions. The limited size of the tank influenced ice formation, including the scales of observable features. Near the tank walls, less bubbling allowed ice to form more easily - an effect which could occur at contact surfaces in nature - although it never fully adhered to the side walls. The chamber pressure (~4.5 mbar) was higher than the extremely low pressures on icy moons (~10^{-16} Pa; Hall et al., 1995); however, the evaporation of substantial amounts of water from cryolavas likely creates localized regions of elevated pressure above cryovolcanic eruptions (Porco et al., 2006; see also pressure fluctuations during boiling in Bargery et al., 2010, and Raposa et al., 2024).

Our experiments were designed to study processes in the upper centimetres of a water column. In natural effusions, liquid water in contact with a cold planetary surface would likely also freeze at its base, potentially inducing cold currents to rise from depth and stir the liquid at different spatial wavelengths to rising bubbles; the ice/water density contrast would also increase pressure of the confined liquid. These phenomena likely reduce ice lid stability further and alter the resulting ice morphology. Future experiments should account for these effects.

Unfortunately, the ice melted before we could examine its interior, preventing direct analyses of its internal structure. The videos (available in low resolution in Supplementary material or in high-resolution on Zenodo, Brož et al., 2025) do not suggest a snow-like, honeycomb, or frazil structure for the ice. However, given that freezing occurred alongside boiling, and the prior findings of Brož et al. (2023) who investigated the inflation of viscous muds due to boiling, we hypothesize that the ice was porous.

Another limitation of our setup is that it uses confined, stationary liquid water rather than flowing cryolava. While it captures boiling, freezing, and ice disruption under low pressure, it cannot simulate large-scale dynamics like radial spreading or downslope flow. Such motions might stress forming ice crusts (e.g., Morrison et al., 2022) more than boiling alone. Our results thus offer a close-up view of the freezing–boiling interface, but should be cautiously applied to natural cryovolcanic flows.

Finally, as we do not know the specific compositions of cryolavas, it is difficult to estimate the appropriate salt(s) species and concentrations for the experiments. Salts variably affect phase transitions due to their influence on freezing and boiling points (e.g. Vrbka and Jungwirth, 2007; Poston et al., 2024). The effect of salts on the flow of a liquid water-clay mixture was studied by Krýza et al. (2025), who demonstrated experimentally that salt presence can significantly alter the way brine mixtures flow. Again, however, their experiments used only small liquid volumes (~500 ml).

4.2. Implications

The stability of liquid water on Earth is anomalous amongst contemporary planetary surfaces in the Solar System, where vacuum-like or low-pressure conditions below the triple point of water are common. Our observations suggest that liquid water freezing in such environments is more complex than previously assumed; solidification may take longer than proposed (e.g., Quick et al., 2017) due to repeated disruption of the forming ice layer by boiling. Our experiments also suggest that the morphology and thickness of the ice layer would differ from those formed over water bodies on Earth. Cryolava flow morphologies likely also differ from terrestrial lava flows due to the effect of liquid water instability on their behaviour and propagation.

Additionally, we observe that fracturing and vapour accumulation beneath an ice layer creates an uneven, likely porous surface with bumps and depressions a few centimetres in height. While too small to detect in visible-light images, such features could influence radar reflections, thus offering the future possibility to detect effusive cryolavas on icy moons. Our findings are also relevant for Mars where atmospheric pressure is below the triple point of water, providing new insights into how liquid water might have behaved through the Amazonian Period (3 Ga–present; e.g. Gallagher and Balme, 2015; Butcher et al., 2020), since Mars lost most of its atmosphere.

Acknowledgements

This work was funded by the Czech Grant Agency grant No. 25-15473S. Chamber access was provided by project CZ.02.2.69/0.0/0.0/18_053/0016986 of the Ministry of Education, Youth and Sports of the Czech Republic. We acknowledge support from Charles University Research Centre program No. UNCE/24/SCI/005 (VP), a Leverhulme Trust Early Career Fellowship (FB), and UK Space Agency funding grants ST/X006549/1, ST/Y000234/1 and ST/Y006054/1 (MP). We thank the two anonymous reviewers for their constructive and critical feedback, which helped improve the quality of this manuscript. We also acknowledge Olivier Mousis for handling the editorial process.

References

Ahrens, C. J., 2020, Modeling cryogenic mud volcanism on Pluto. *Journal of Volcanology and Geothermal Research*, 406, 107070, https://doi.org/10.1016/j.jvolgeores.2020.107070.

Allison, M.L., and Clifford, S.M., 1987, Ice-covered water volcanism on Ganymede, *Journal of Geophysical Research*, v. 92, p. 7865–7876, https://doi.org/10.1029/JB092iB08p07865.

Ashton, G.D., 1986, River and lake ice engineering: Littleton, Colorado, Water Resources Publications.

Bargery, A.S., Lane, S.J., Barrett, A., Wilson, L., and Gilbert, J.S., 2010, The initial responses of hot liquid water released under low atmospheric pressures: Experimental insights: *Icarus*, v. 210, p. 488–506, https://doi.org/10.1016/j.icarus.2010.06.019.

Brož, P., Krýza, O., Conway, S.J., Mueller, N.T., Hauber, E., Mazzini, A., Raack, J., Patel, M.R., Balme, M.R., and Sylvest, M.E., 2020a, Mud flow levitation on Mars: Insights from laboratory simulations: *Earth and Planetary Science Letters*, v. 545, https://doi.org/10.1016/j.epsl.2020.116406.

Brož, P., Krýza, O., Wilson, L., Conway, S. J., Hauber, E., Mazzini, A., Raack, J., Patel, M.R., Balme, M.R., and Sylvest, M.E., 2020b, Experimental evidence for lava-like mud flows under Martian surface conditions. Nature Geoscience, 13(6), 403–407. https://doi.org/10.1038/s41561-020-0577-2

Brož, P., Krýza, O., Patočka, V., Pěnkavová, V., Conway, S.J., Mazzini, A., Hauber, E., Sylvest, M.E., and Patel, M., 2023, Volumetric changes of mud on Mars: Evidence from laboratory simulations: *Journal of Geophysical Research: Planets*, v. 128, e2023JE007950, https://doi.org/10.1029/2023JE007950.

Brož, P., Patočka, V., Butcher, F., Sylvest M., Patel, M., 2025, Movies, temperature and pressure measurements associated with the study ”The complexity of water freezing under reduced atmospheric pressure”, Zenodo, https://zenodo.org/records/14639337.

Butcher, F.E.G., Balme, M.R., Conway, S.J., Gallagher, C., Arnold, N.S., Storrar, R.D., Lewis, S.R., and Hagermann, A., 2020, Morphometry of a glacier-linked esker in NW Tempe Terra, Mars, and implications for sediment-discharge dynamics of subglacial drainage, *Earth and Planetary Science Letters,* v. 542, 116325, https://doi.org/10.1016/j.epsl.2020.116325

Fagents, S.A., 2003, Considerations for effusive cryovolcanism on Europa: The post-Galileo perspective: *Journal of Geophysical Research*, v. 108, 5139.

Gallagher, C., and Balme, M, 2015, Eskers in a complete, wet-based glacial system in the Phlera Montes region, Mars, *Earth and Planetary Science Letters,* v. 431, p. 96-109, https://doi.org/10.1016/j.epsl.2015.09.023

Hall, D., Strobel, D., Feldman, P., McGrath, M., and Weaver, H., 1995, Detection of an oxygen atmosphere on Jupiter's moon Europa: *Nature*, v. 373, p. 677.

Hendrix, A.R., Hurford, T.A., Barge, L.M., Bland, M.T., Bowman, J.S., Brinckerhoff, W., Buratti, B.J., Cable, M.L., Castillo-Rogez, J., Collins, G.C., Diniega, S., German, C.R., Hayes, A.G., Hoehler, T., Hosseini, S., Howett, C.J.A., McEwen, A.S., Neish, C.D., Neveu, M., Nordheim, T.A., Patterson, G.W., Patthoff, D.A., Phillips, C., Rhoden, A., Schmidt, B.E., Singer, K.N., Soderblom, J.M., and Vance, S.D., 2019, The NASA roadmap to ocean worlds: *Astrobiology*, v. 19, p. 1–22, https://doi.org/10.1089/ast.2018.1955.

Kargel, J.S., 1994, Cryovolcanism on the icy satellites. *Earth Moon Planet* **67**, 101–113, https://doi.org/10.1007/BF00613296.

Kirk, R., Soderblom, L., Brown, R., Kieffer, S., and Kargel, J., 1995, Triton's plumes: Discovery, characteristics, and models, in Cruikshank, D.P., Matthews, M.S., and Schumann, A.M., eds., *Neptune and Triton*: Tucson, Arizona, University of Arizona Press, v. 1, p. 949–989.

Küppers, M., et al., 2014, Localized sources of water vapor on the dwarf planet (1) Ceres: *Nature*, v. 505, p. 525–527.

Krýza, O., Brož, P., Fox-Powell, M., Pěnkavová, V., Conway, S., Mazzini, A., Hauber, E., Sylvest, M., Patel, M., (2025). Small amounts of dissolved salts increase the mobility of mud flows on Mars and other extraterrestrial bodies. *Commun Earth Environ* 6, 116, https://doi.org/10.1038/s43247-025-02110-w.

Lesage, E., Schmidt, F., Andrieu, F., and Massol, H., 2021, Constraints on effusive cryovolcanic eruptions on Europa using topography obtained from Galileo images: *Icarus*, v. 361, 114373, https://doi.org/10.1016/j.icarus.2021.114373.

Lopes, R., Mitchell, K., Stofan, E., Lunine, J., Lorenz, R., Paganelli, F., Kirk, R., Wood, C., Wall, S., Robshaw, L., et al., 2007, Cryovolcanic features on Titan's surface as revealed by the Cassini Titan Radar Mapper: *Icarus*, v. 186, p. 395–412.

McGovern, P. J., White, O. L., & Schenk, P. M., 2021, Tectonism and enhanced cryovolcanic potential around a loaded Sputnik Planitia basin, Pluto. *Journal of Geophysical Research: Planets, 126*(11), e2021JE006964, https://doi.org/10.1029/2021JE006964.

Morrison, A.A., Whittington, A.G., and Mitchell, K.L., 2022, A reevaluation of cryolava flow evolution: Assumptions, physical properties, and conceptualization: *Journal of Geophysical Research: Planets*, v. 128, https://doi.org/10.1029/2022JE007383.

Porco, C.C., Helfenstein, P., Thomas, P.C., Ingersoll, A.P., Wisdom, J., West, R., Neukum, G., Denk, T., Wagner, R., Roatsch, T., Kieffer, S., Turtle, E., McEwen, A., Johnson, T.V., Rathbun, J., Veverka, J., Wilson, D., Perry, J., Spitale, J., Brahic, A., Burns, J.A., Del Genio, A.D., Dones, L., Murray, C.D., and Squyres, S., 2006, Cassini observes the active south pole of Enceladus: *Science*, v. 311, p. 1393–1401, https://doi.org/10.1126/science.311.5766.1393.

Poston, M.J., Baker, S.R., Scully, J.E.C., Carey, E.M., McKeown, L.E., Castillo-Rogez, J.C., and Raymond, C.A., 2024, Experimental examination of brine and water lifetimes after impact on airless worlds: *The Planetary Science Journal*, v. 5, https://doi.org/10.3847/PSJ/ad696a.

Raposa, S.M., Engle, A.E., Tan, S.P., Grundy, W.M., Hanley, J., Lindberg, G.E., Umurhan, O.M., Steckloff, J.K., Thieberger, C.L., and Tegler, S.C., 2024, Outbursts upon cooling of low-temperature binary mixtures: Experiments and their planetary implications: *Journal of Geophysical Research: Planets*, https://doi.org/10.1029/2024JE008457.

Quick, L.C., Glaze, L.S., and Baloga, S.M., 2017, Cryovolcanic emplacement of domes on Europa: *Icarus*, v. 284, p. 477–488.

Roth, L., et al., 2014, Transient water vapor at Europa's south pole: *Science*, v. 343, p. 171–174, https://doi.org/10.1126/science.1247051.

Ruesch, O., Genova, A., Neumann, W., Quick, L.C., Castillo-Rogez, J.C., Raymond, C.A., and Zuber, M.T., 2019, Slurry extrusion on Ceres from a convective mud-bearing mantle: *Nature Geoscience*, v. 12, p. 505–509.

Strom, R.G., 1986, The solar system cratering record: Voyager 2 results at Uranus and implications for the origin of impacting objects, Icarus 70, 517-535, https://doi.org/10.1016/0019-1035(87)90093-5.

Sparks, W.B., Schmidt, B.E., McGrath, M.A., Hand, K.P., Spencer, J.R., Cracraft, M., and Deustua, S.E., 2017, Active cryovolcanism on Europa? *The Astrophysical Journal*, v. 839, L18, https://doi.org/10.3847/2041-8213/aa67f8.

Umurhan, O. M., Ahrens, C. J., and Chevrier, V. F., 2021, Rheological and thermophysical properties and some processes involving common volatile materials found on Pluto's surface. *The Pluto System After New Horizons*, 195-255, ISBN: 9780816540945.

Vrbka, L., and Jungwirth, P., 2007, Molecular dynamics simulations of freezing of water and salt solutions: *Journal of Molecular Liquids*, v. 134, p. 64–70. https://doi.org/10.1016/j.molliq.2006.12.011.